Phytotaxa 489 (2): 121–139
https://www.mapress.com/j/pt/

Article

ISSN 1179-3155 (print edition)
PHYTOTAXA
ISSN 1179-3163 (online edition)

https://doi.org/10.11646/phytotaxa.489.2.2

Pseudopestalotiopsis gilvanii sp. nov. and *Neopestalotiopsis formicarum* leaves spot pathogens from guarana plant: a new threat to global tropical hosts

GILVANA F. GUALBERTO[a,e], ARICLÉIA DE M. CATARINO[a,f], THIAGO F. SOUSA[b,c,g], JEFERSON C. CRUZ[c,h], ROGÉRIO E. HANADA[a,i], FERNANDA F. CANIATO[d,j] & GILVAN F. SILVA[c,k]*

[a] *Programa de Pós-Graduação em Agricultura no Trópico Úmido, INPA, Manaus, 69.060-001 Brasil.*
[b] *Department of Microbiology, Federal University of Viçosa (UFV), Viçosa 36570-900, Brazil.*
[c] *Embrapa Amazônia Ocidental, Manaus 69010-970, Brazil.*
[d] *Department of Fundamental Sciences and Agricultural Development, Faculty of Agricultural Sciences, Federal University of Amazonas (UFAM), Manaus 69080-900, Brazil.*
[e] *gilvanafigueira43@gmail.com; https://orcid.org/0000-0001-7124-8335*
[f] *amoraescatarino@gmail.com; https://orcid.org/0000-0002-5579-8625*
[g] *thiago-fernandes2@hotmail.com; http://orcid.org/0000-0002-7451-9839*
[h] *jeferson.cruz@embrapa.br; https://orcid.org/0000-0002-7718-2127*
[i] *rhanada.inpa@gmail.com; https://orcid.org/0000-0002-4544-4882*
[j] *fernanda.f.caniato@gmail.com; https://orcid.org/0000-0001-7597-0587*
[k] *gilvan.silva@embrapa.br; https://orcid.org/0000-0003-2828-8299*
**Corresponding author: gilvan.silva@embrapa.br*

Abstract

Pestalotioid species (*Pestalotiopsis*, *Pseudopestalotiopsis* and *Neopestalotiopsis*) cause extremely damaging diseases in a wide range of hosts across the word. Recently, pestalotioid strains isolated from damaged guarana leaf tissue were subject to morphological and molecular characterization. Six monosporic isolates were obtained and analysed based on the following conidial characters: length, width, septation, absence or presence of basal appendage, number and length of apical appendages. For phylogenetic inference, sequences of the Internal Transcribed Spacer region (ITS), partial sequences of the genes encoding the translation elongation factor 1-α (*tef1-α*) and β-tubulin (*tub2*) were used. Three out of six strains analysed were identified as *Neopestalotiopsis formicarum,* while the three other isolates are described here as a new species of *Pseudopestalotiopsis,* named *Ps. gilvanii sp. nov.*. The pathogenicity of *N. formicarum* and *Ps. gilvanii* were confirmed following Koch's postulate. Besides guarana, the potential of *N. formicaram* and *Ps. gilvanii* to cause diseases in other economically important tropical plants were investigated. *Ps. gilvanii* was pathogenic to açaí palms (*Euterpe oleracea, E. precatoria*), and oil palm (*Elaeis guineensis*), but not to banana (*Musa paradisiaca* var. *pacovan*) and rubber trees (*Hevea brasiliensis*). *N. formicarum* was not pathogenic to rubber trees but was pathogenic to other species tested. To our knowledge this is the first report of *N. formicarum* as a plant pathogen in the guarana plant, and *Ps. gilvanii* as novel plant pathogen capable of causing disease in important plant crops from tropical regions.

Keywords: Pestalotiopsis-like, açaí palm, oil palm, banana, plant pathogen, and leaf spot

Introduction

The guarana plant [*Paullinia cupana* var. *sorbilis*, (Mart.) Ducke] is a native species of the Brazilian Amazon, whose seeds possess therapeutics, medicinal and pharmacological properties as cytoprotective modulators of antioxidant enzyme activities, anxiolytic, panicolytic, antibacterial and antineoplastic effects (Bonadiman *et al.* 2017; Carvalho *et al.* 2016; Rangel *et al.* 2013; Silveira *et al.* 2018). Moreover, the high concentration of caffeine in guarana seeds make them attractive to the beverage industry (Beaufort 2018).

Brazil is the only country where guarana is cultivated on a commercial scale, however, phytosanitary issues have limited the yield of the guarana crop and its expansion, especially in the State of Amazonas, where climatic features such as high humidity combined with high temperature, favors the proliferation of fungal diseases. Two main diseases affecting guarana yield can be highlighted: oversprouting caused by *Fusarium decemcellulare* and anthracnose caused

Accepted by Ruvishika Jayawardena: 31 Dec. 2020; published: 4 Mar. 2021

by *Colletotrichum guaranicola* (Queiroz *et al.* 2020). Until now, *C. guaranicola* was the only known pathogen causing anthracnose-like leaf spots in the guarana plant. However, during a survey conducted to anthracnose-like leaf spots in a guarana field near the municipality of Manaus, two pathogens of the genus *Neopestalotiopsis* and *Pseudopestalotiopsis,* were identified instead *C. guaranicola,* and were reported in the current study.

Pestalotiopsis (Steyaert, 1949) is a member of the family Amphisphaeriaceae. This genus comprises about 374 species (Index Fungorum; http://www.indexfungorum.org/Names/Names.asp). The morphology of conidia among *Pestalotiopsis* has been described as fusiform, ellipsoid, straight or slightly curved, with five cells, containing three brown median cells and two hyaline cells (apical and basal), with two or more apical appendages (Jeewon *et al.* 2002; Maharachchikumbura *et al.* 2014). Even in 2003, combining characteristics of median cells with ITS region analysis, the first evidence came up that members of *Pestalotiopsis* should not be considered a single taxon (Jeewon *et al.* 2003). It was only in 2014 that taxonomic reorganization of the *Pestalotiopsis* was proposed by the adoption of multilocus phylogeny of ITS, *tub2 and tef1-α* regions in combination with characteristics related to the morphology of conidia, such as the color of median cells and conidiogenous cells. At that time, *Neopestalotiopsis* and *Pseudopestalotiopsis* were introduced (Maharachchikumbura *et al.* 2014). Currently, 23 species of *Pseudopestalotiopsis* and 47 species of *Neopestalotiopsis* have been reported (Index Fungorum).

Representative species of *Pestalotiopsis*, *Pseudopestalotiopsis* and *Neopestalotiopsis,* have been reported as endophytic (Alade *et al.* 2018; Yu *et al.* 2020; Zhou *et al.* 2018), saprophytes (Costa & Gusmão 2015; Jeewon *et al.* 2013; Maharachchikumbura *et al.* 2014), and causal agents of disease, in the fruits and leaves of important economic plants, such as *Fragaria ananassa*, *Vitis vinifera*, *Euterpe oleracea, Camellia sinensis* L., *Eucalyptus* spp., *Hevea brasiliensis, Mangifera indica, Camellia chrysantha* (Ayoubi & Soleimani 2016; Jayawardena *et al.* 2016; Morales-Rodríguez *et al.* 2019; Pornsuriya *et al.* 2020; Shu *et al.* 2020; Zhao *et al.* 2020) and other plant species, such as fishtail palm (*Caryota mitis*), white heather (*Erica arborea*), and *Bulbophyllum thouars* (Catarino *et al.* 2020; Hlaiem *et al.* 2018; Wang *et al.* 2017).

In *Camellia sinensis*, species from three genera (*Pseudopestalotiopsis camelliae-sinensis*, *Neopestalotiopsis clavispora* and *Pestalotiopsis camelliae*) were associated with gray blight symptoms (Chen *et al.* 2018). The pestalotioid group (*Pestalotiopsis*, *Pseudopestalotiopsis* and *Neopestalotiopsis*) cause diseases in a wide range of hosts around the world. However, despite its capability to cause losses in economically important crops, it has not yet been properly recognized (Ayoubi & Pari 2016).

Although agronomic losses have been associated with diseases caused by pestalotioid species, their biotechnological potential has also been described. Before taxonomic reformulation, a set of 135 compounds were reported in a review focused in *Pestalotiopsis*, summarizing the main activities related to secondary metabolites as antiviral, antibacterial, antifungal and antitumor activities (Xu *et al.* 2010). Recently eight new polyketides derived from *Pseudopestalotiopsis theae* have been identified, some of them displaying activity against drug-resistant bacteria (Yu *et al.* 2020), in addition to, compounds with cytotoxic and antimicrobial effects (Alade *et al.* 2018; Riga *et al.* 2019; Yuan *et al.* 2017).

Several other substances of medical and industrial importance have been isolated from pestalotioid fungi, such as taxol (Kathiravan *et al.* 2014), furanones (Liu *et al.* 2012, chitin deacetylase (Cord-Landwehr *et al.* 2016), chlorinated chromone and diphenyl ether derivatives (Klaiklay *et al.* 2012). Besides that, important environmental applications have also been observed in pestalotioid fungi (Marzall-Pereira *et al.* 2019). Russell *et al.* (2011) described two *Pestalotiopsis microspora* endophytic isolates with the ability to use polyurethane as their only carbon source, showing the potential of this endophytic for bioremediation.

Recently, 13 new pestalotioid species were described: five *Pseudopestalotiopsis*, six *Neopestalotiopsis* and two *Pestalotiopsis* (Norphanphoun *et al.* 2019; Tsai *et al.* 2020). Here we introduce *Pseudopestalotiopsis gilvanii sp. nov.,* a new phytopathogenic species isolated from guarana plants, and the first report of *Neopestalotiopsis formicarum* as a pathogen in the guarana plant. The host range was further evaluated on five important commercial crops of tropical regions.

Material and methods

Isolation and culture conditions

Leaves showing irregular dark brown spots were sampled in guarana fields near the municipality of Manaus (2°53’28. 6” S 59°58’35. 6” W) and brought to the laboratory. The tissues were fragmented and surface sterilized with alcohol

70% (v/v) for one minute, sodium hypochlorite 0.2% (v/v) for three minutes, and washed with sterilized distilled water for three minutes. The fragmented leaves were then incubated in PDA medium (200 g L^{-1} potato, 15 g L^{-1} agar, 20 g L^{-1} dextrose and 100 mg L^{-1} chloramphenicol) at 25 °C for three days. The monosporic isolates obtained were used for morphological and molecular characterization, as well as, pathogenicity assays. The isolates accessions were registered at Sistema Nacional de Gestão do Patrimônio Genético e do Conhecimento Tradicional Associado (SisGen, Brazil, Registration Nº A6FB8EF). The holotype and ex-type living cultures of the new species from this study were deposited in the Microbiological Collections of the National Institute of Amazon Research (INPA).

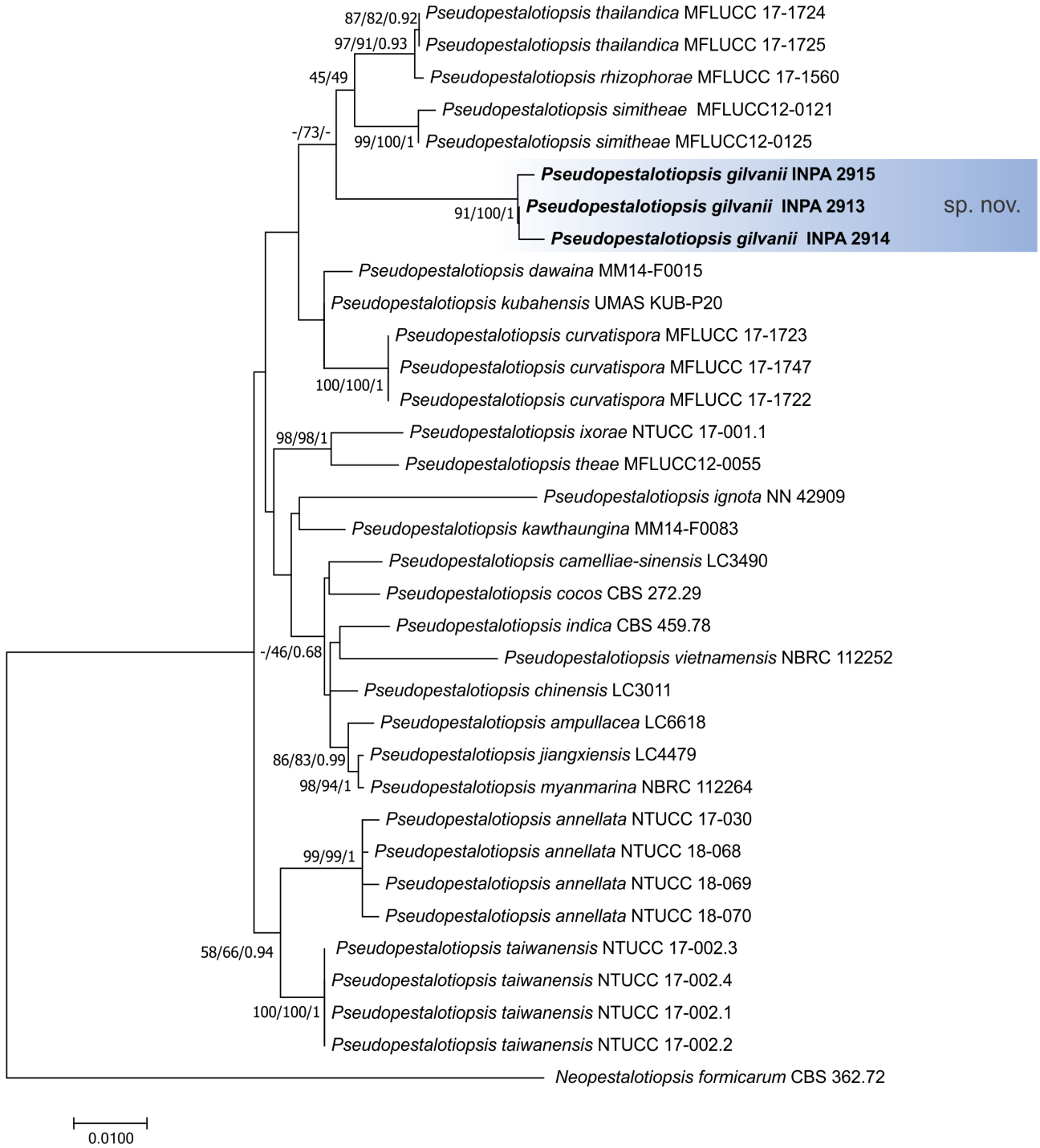

FIGURE 1. Phylogenetic relationship in *Pseudopestalotiopsis* inferred with concatenated sequences of ITS, *tub2* and *tef1-α*, showing the placement *Pseudopestalotiopsis gilvanii*. The tree topology was generated by the ML analysis and bootstrap values for maximum parsimony (MP), maximum likelihood (ML), and posterior probability (PP) analyses are presented at the branches (MP/ML/PP). Isolates from this study are highlighted in blue.

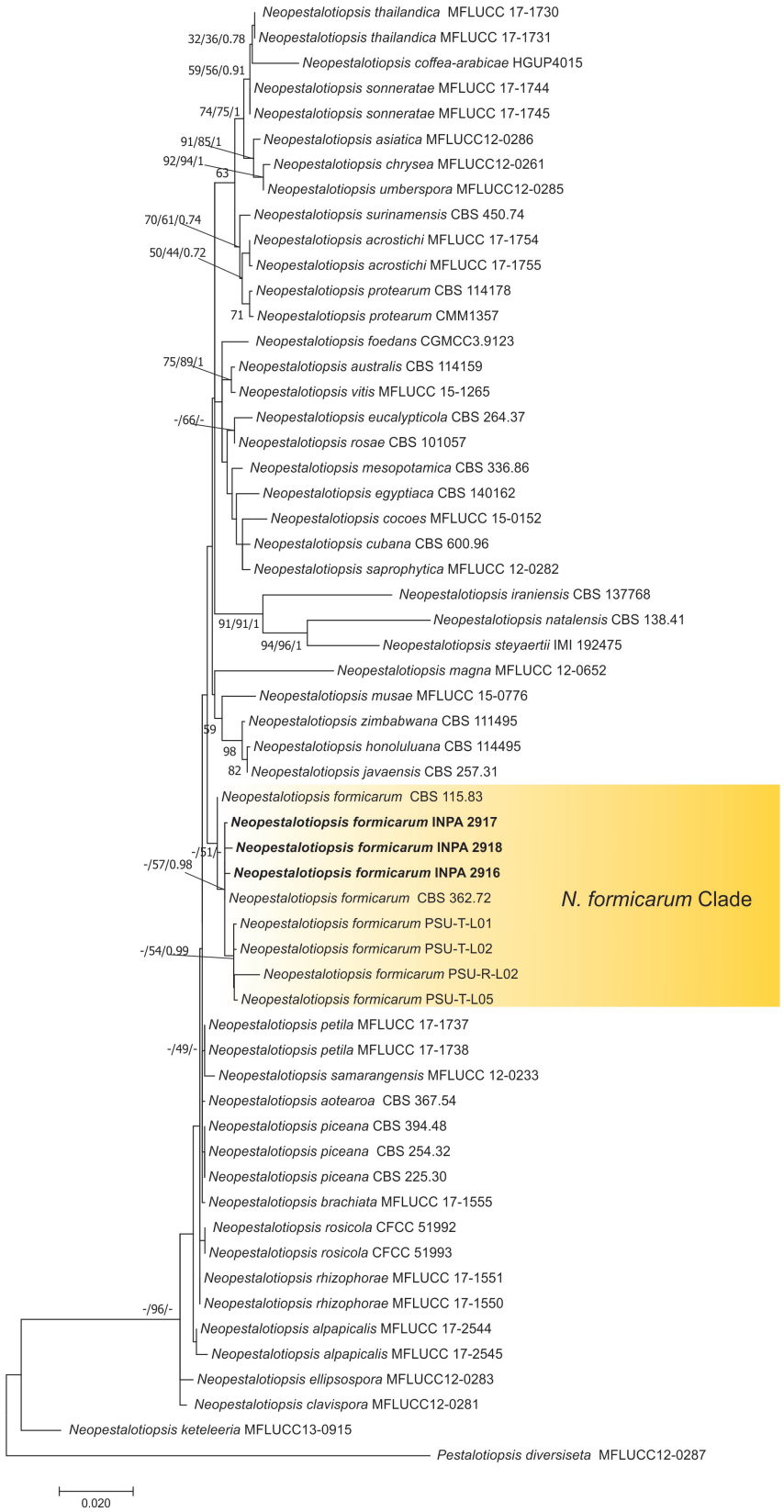

FIGURE 2. Phylogenetic relationship in *Neopestalotiopsis* inferred with concatenated sequences of ITS, *tub2* and *tef1-α.* The tree topology was generated by the ML analysis and bootstrap values for maximum parsimony (MP), maximum likelihood (ML), and posterior probability (PP) analyses are presented at the branches (MP/ML/PP). Isolates from this study are highlighted in yellow.

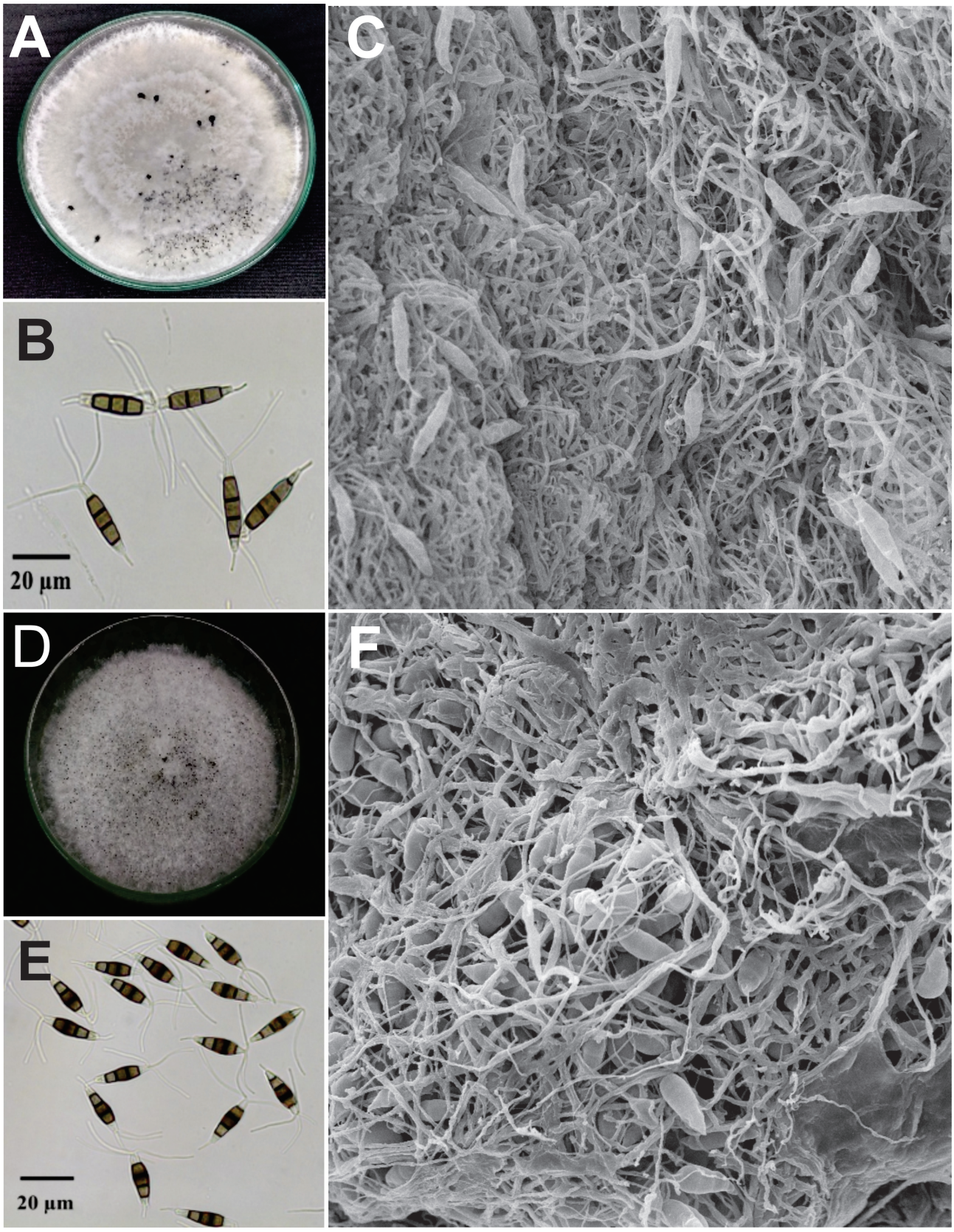

FIGURE 3. *Pseudopestalotiopsis gilvanii* (strain INPA 2913), aspects of colonies in PDA (A), aspects of conidia (B) and scanning electron microscopy of conidia (C). *Neopestalotiopsis formicarum* (strain INPA 2916), aspects of colonies in PDA (D), aspects of conidia (E) and scanning electron microscopy of conidia (F).

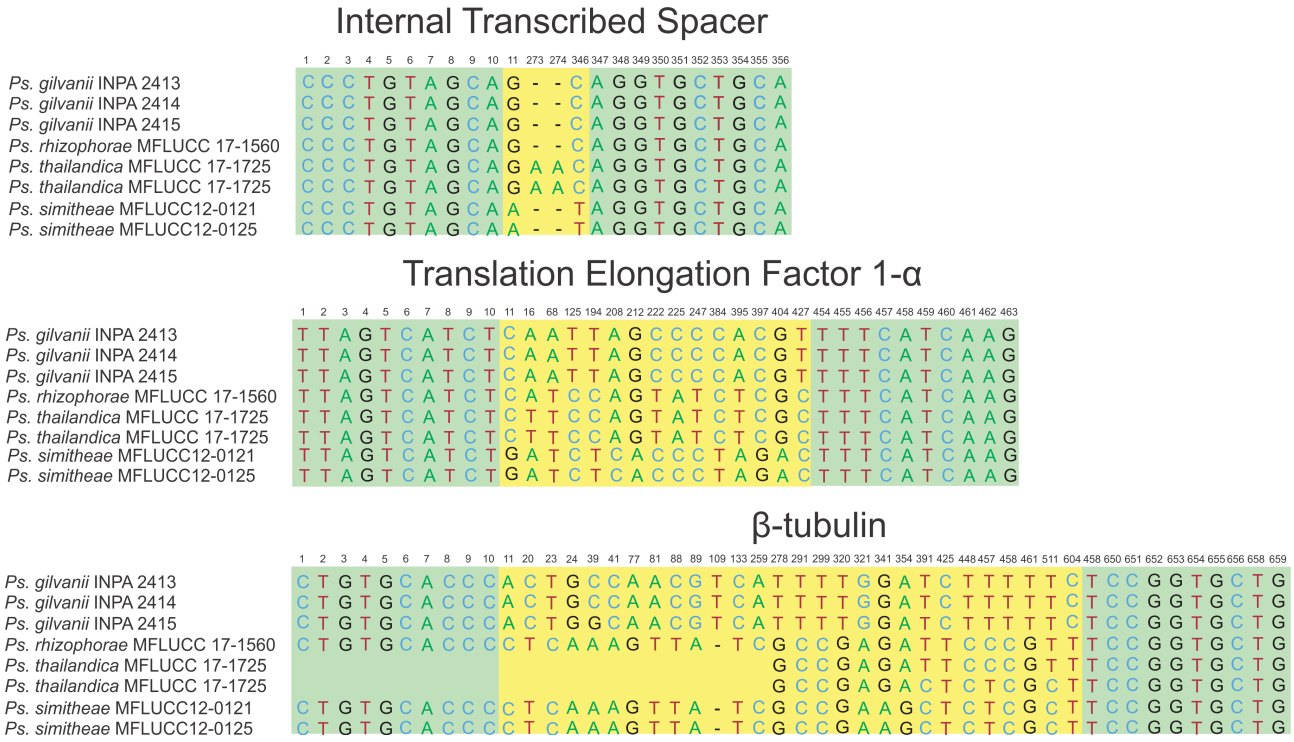

FIGURE 4. Nucleotides differences in the ITS, *tef1-α* and *tub2* sequences of *Pseudopestalotiopsis gilvanii* and closely related species. Ten nucleotides up and downstream to the nucleotide variation are in light green.

Morphology and morpho-cultural aspects of colonies

Each isolate was grown in PDA medium for 10 days when the following morphological variables of conidia were taken: length (in µm), width (in µm), septation, absence or presence of basal appendage, number and length of apical appendages (in µm). The pigment of the median cells was also recorded and classified neither as "concolor" if median cells showed uniform pigmentation or "versicolor" if median cells showed non-uniform pigmentation. The appearance of the colonies was classified according to their color and type of mycelium. For each isolate, one hundred conidia were used to measure its length and width using Carl ZEISS Axio Imager v2.

Scanning electron microscopy (SEM) was used to fine examine the structures of the spores and inoculated leaves. Samples of isolates grown in PDA medium and those obtained by inoculation of conidia in healthy guarana plants were pre-fixed in 2.5% glutaraldehyde (9:1, v/v) for 2 hrs followed by dehydration in ethyl alcohol at concentrations of 50%, 70%, 90%, 95%, and 100% (v/v) for 10 to 15 min, then placed in Critical Point Drying (Baltec-CPD-030) for complete drying. Samples were assembled in the sample holder of the scanning electron microscope with double-sided carbon tape and submitted to metalization with gold and visualized under a scanning electron microscope (Model 435, VP Leo Electronics Systems, Cambridge, UK).

DNA extraction and PCR conditions

The monosporic isolates were grown in enriched PD medium (200 g L^{-1} potato extract, 10 g L^{-1} dextrose, 2 g L^{-1} yeast extract, 2 g L^{-1} peptone, 1.5 g L^{-1} casein) to obtain the mycelial mass. The mycelial mass obtained was vacuum-filtered and stored at -80 °C. Total DNA was isolated from approximately one gram of mycelial mass following the CTAB method (Doyle & Doyle 1990). The DNA isolated was quantified using a spectrophotometer (ND-2000, NanoDrop Technologies, Wilmington, DE, USA) and its integrity inspected in agarose gel 0.8% (m/v).

Primers that amplified fragments of encoding the translation elongation factor 1-α (*tef1-α*), β-tubulin (*tub2*) and internal transcribed spacer (ITS) were used for phylogenetic analysis (Table 1). PCR amplifications were performed in a final volume of 25 µl containing: 150 ng of the total DNA; 0.5 pmol of each primer; 1X reaction buffer (100 mM Tris-HCl (pH 8.8 at 25 °C), 500 mM KCl, 0.8% (v/v) Nonidet P40); 2 mM $MgCl_2$; 1 mM dNTPs and 1 U of Taq polymerase (DNA Express). PCR amplifications consisted of initial denaturation at 94 °C for 3 min, 40 cycles of denaturation at 94 °C for 1 min, annealing according to each primer-specific temperature (Table 1) for 30 secs, elongation at 72 °C

for 1 min and 30 secs. Final elongation was performed at 72 °C for 5 min. To confirm the amplification of the target sequences, the PCR products were resolved in agarose gel 1.5 % (m/v), stained with ethidium bromide and then photographed under UV light on a Molecular Imaging System (Loccus Biotecnologic L-Pix. Chemi) and compared with a 1 kb ladder (Invitrogen).

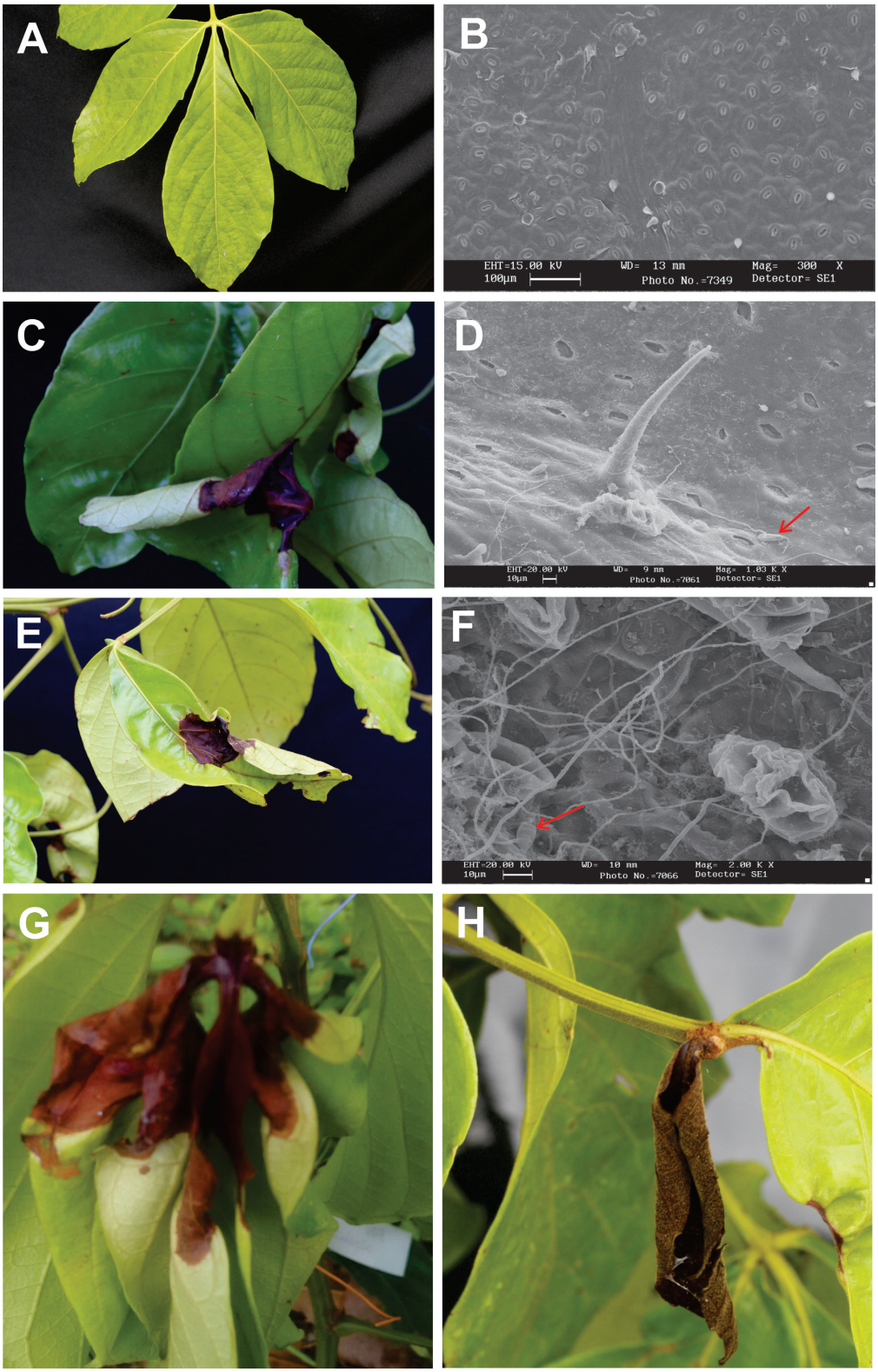

FIGURE 5. Pathogenicity assay on guarana plants. Negative control showing absence of symptoms (A) and scanning electron microscopy of control (B). Symptoms of leaf spot caused by *Pseudopestalotiopsis gilvanii,* strain INPA 2913 (C) and scanning electron microscopy of inoculated leaf showing conidia, red arrow (D). Symptoms of leaf spot caused by *Neopestalotiopsis formicarum,* strain INPA 2016 (E) and scanning electron microscopy of inoculated leaf showing conidia, red arrow (F), fall of the leaves caused by *Ps. gilvanii* (G) and *N. formicarum* (H).

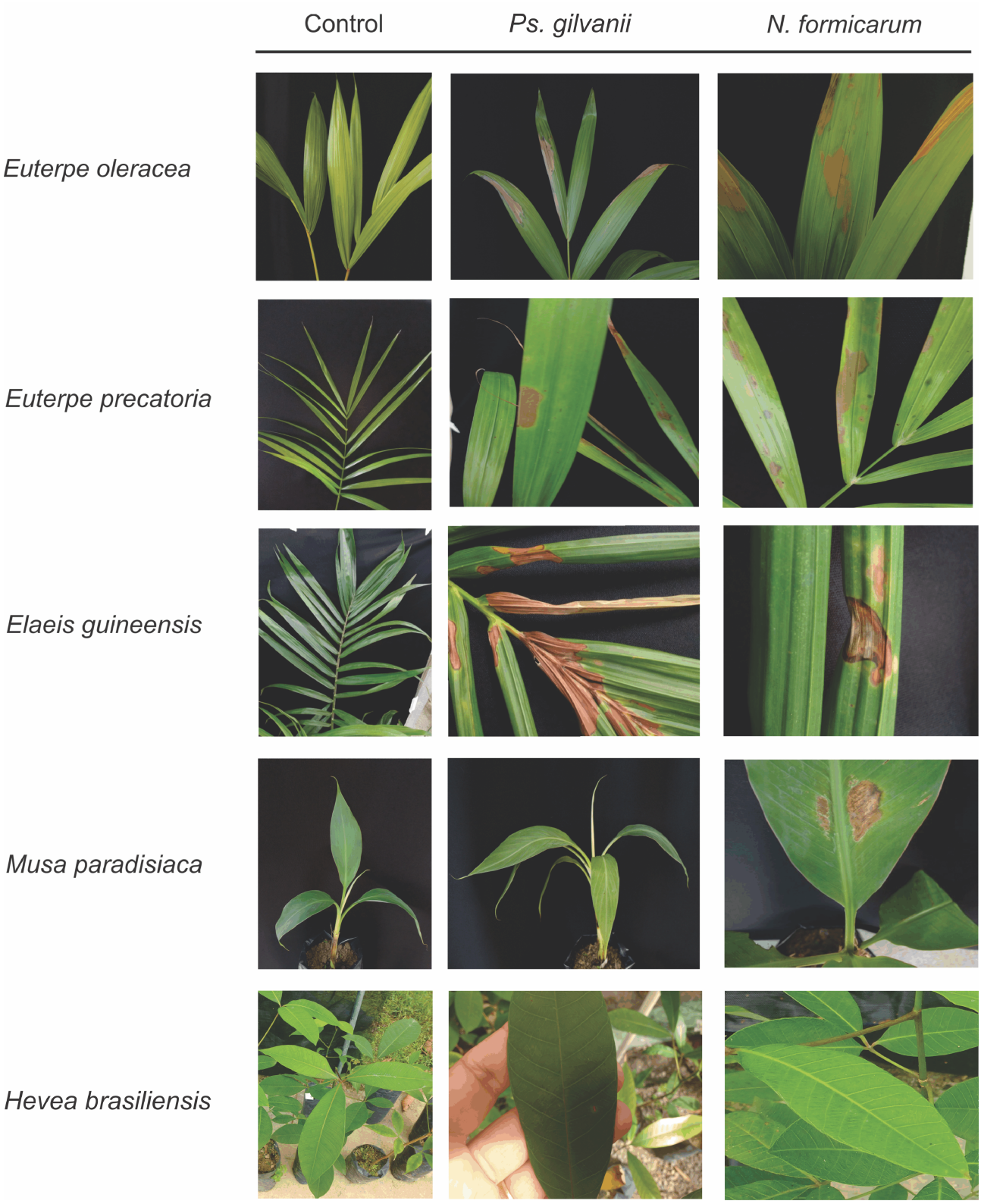

FIGURE 6. Leaf spot symptoms on tropical plants inoculated with *Pseudopestalotiopsis gilvanii* and *Neopestalotiopsis formicarum*, under greenhouse conditions. Presence of symptoms noticed on açaí palms (*Euterpe oleraceae and E. precatoria*), oil palm (*Elaeis guineenses*). Banana (*Musa paradisiaca*) displayed symptoms for *N. formicarum* but not for *Ps. gilvanii.* Absence of symptoms on rubber trees *(Hevea brasiliensis*). Uninoculated plants were employed as control.

TABLE 1. Characteristics of the primers used for phylogenetic analysis in this study.

Locus	Primer/ Direction	Primer sequence 5' to 3'	References	AT	Amplicon
Nuclear ITS 5.8S and 18S partial rDNA	ITS1/F	TCCGTAGGTGAACCTGCGG	(White *et al.* 1990)	55 °C	600~
	ITS4/R	TCCTCCGCTTATTGATATGC			
β-tubulin (*tub2*)	T1/F	AACATGCGTGAGATTGTAAGT	(O'Donnell & Cigelnik 1997)	57 °C	800~
	Bt-2b/R	ACCCTCAGTGTAGTGACCCTTGGC	(Glass & Donaldson 1995)		
Translation elongation factor 1-α (*tef1-α*)	EF1-728/F	CATCGAGAAGTTCGAGAAGG	(Carbone & Kohn 1999)	54 °C	500~
	EF-2/R	GGA(G/A)GTACCAGT(G/C)ATCATGTT	(O'Donnell *et al.* 1998)		

Sequencing, Alignment and Phylogenetic analyzes

PCR products were treated with a 20% (m/v) polyethylene glycol solution (PEG) and then used for sequencing reactions that were carried out in a final volume of 10 µl containing: 5 µl of purified PCR products, 2 µl of Big Dye v3.1 (Thermo Fisher), 2 µl of 5X buffer (Applied Biosystems) and 3.2 pmol of each primer. Sequencing reactions proceeded at 96 °C for 4 min, followed by 30 cycles at 96 °C for 10 sec, 50 °C for 5 sec and 60 °C for 4 min. Sequencing reactions were analysed on a 3500 Genetic Analyzer Sequencer (Thermo Fisher).

Consensus sequences were obtained based on the alignment of both forward and reverse sequences using DNA baser assembly software (http://www.dnabaser.com/). The new sequences obtained were deposited in GenBank (http://www.ncbi.nlm.nih) under the accession numbers of Table 2.

TABLE 2. Species of *Pseudopestiopsis* and *Neopestalotiopsis* used for phylogenetic analyses in this study, strain number, their host, country and GenBank accession numbers. Generated accessions are marked in bold.

Species	Strain number	Host	Country	ITS	*tub2*	*tef1-α*
Ps. gilvanii	**INPA 2913** [a]	***Paullinia cupana***	**Brazil**	**MN385951**	**MN385957**	**MN385954**
Ps. gilvanii	**INPA 2914** [a]	***Paullinia cupana***	**Brazil**	**MN385952**	**MN385958**	**MN385955**
Ps. gilvanii	**INPA 2915** [a]	***Paullinia cupana***	**Brazil**	**MN385953**	**MN385959**	**MN385956**
Ps. annellata	NTUCC 17-030	*Camellia sinensis*	Taiwan	MT322087	MT321889	MT321988
Ps. annellata	NTUCC 18-068	*Camellia sinensis*	Taiwan	MT322089	MT321891	MT321990
Ps. annellata	NTUCC 18-069	*Camellia sinensis*	Taiwan	MT322090	MT321892	MT321991
Ps. annellata	NTUCC 18-070	*Camellia sinensis*	Taiwan	MT322091	MT321893	MT321992
Ps. curvatispora	MFLUCC 17-1722	*Rhizophora mucronate*	Thailand	MK764288	MK764354	MK764332
Ps. curvatispora	MFLUCC 17-1723	*Rhizophora mucronate*	Thailand	MK764289	MK764355	MK764333
Ps. curvatispora	MFLUCC 17-1747	*Rhizophora mucronate*	Thailand	MK764290	MK764356	MK764334
Ps. rhizophorae	MFLUCC 17-1560	*Rhizophora apiculate*	Thailand	MK764291	MK764357	MK764335
Ps. thailandica	MFLUCC 17-1724	*Rhizophora mucronate*	Thailand	MK764292	MK764358	MK764336
Ps. thailandica	MFLUCC 17-1725	*Rhizophora mucronate*	Thailand	MK764293	MK764359	MK764337
Ps. ampullaceae	LC6618	*Camellia sinensis*	China	KX895025	KX895358	KX895244
Ps. camelliae-sinesis	LC3490	*Camellia sinensis*	China	KX894985	KX895316	KX895202
Ps. chinensis	LC3011	*Camellia sinensis*	China	KX894937	KX895269	KX895154
Ps. cocos	CBS 272.29	*Cocos nucifera*	Java, Indonesia	KM199378	KM199467	KM199553
Ps. dawaina	MM14-F0015	Unknown	Dawei, Myanmar	LC324750	LC324751	LC324752

.....continued on the next page

TABLE 2. (Continued)

Species	Strain number	Host	Country	ITS	*tub2*	*tef1-α*
Ps. ignota	NN 42909	Unknown	-	KU500020	-	KU500016
Ps. indica	CBS 459.78	*Hibiscus rosa-sinensis*	-	KM199381	KM199470	KM199560
Ps. ixorae	NTUCC 17-001.1	*Ixora* sp.	-	MG816316	MG816326	MG816336
Ps. jiangxiensis	LC4479	*Eurya* sp.	China	KX895034	KX895343	KX895229
Ps. kawthaungina	MM14-F0083	Unknown	Kawthaung, Myanmar	LC324753	LC324754	LC324755
Ps. kubahensis	UMAS KUB-P20	*Macaranga* sp.	Sarawak, Malaysia	KT006749	-	-
Ps. myanmarina	NBRC 112264	*Averrhoa carambola*	Dawei, Myanmar	LC114025	LC114045	LC114065
Ps. simitheae	MFLUCC 12-0121	*Pandanus odoratissimus*	Thailand	KJ503812	KJ503815	KJ503818
Ps. simitheae	MFLUCC 12-0125	living leaves of *Pandanus odoratissimus*	Thailand	KJ503813	KJ503816	KJ503819
Ps. taiwanensis	NTUCC 17-002.1	*Ixora* sp.	Taiwan	MG816319	MG816329	MG816339
Ps. taiwanensis	NTUCC 17-002.2	*Ixora* sp.	Taiwan	MG816320	MG816330	MG816340
Ps. taiwanensis	NTUCC 17-002.3	*Ixora* sp.	Taiwan	MG816321	MG816331	MG816341
Ps. taiwanensis	NTUCC 17-002.4	*Ixora* sp.	Taiwan	MG816322	MG816332	MG816342
Ps. theae	MFLUCC 12-0055	*Camellia sinensis*	Thailand	JQ683727	JQ683711	JQ683743
Ps. vietnamensis	NBRC 112252	*Fragaria* sp.	Hue, Vietnam	LC114034	LC114054	LC114074
N. formicarum	**INPA 2916** [a]	***Paullinia cupana***	**Brazil**	**MN267737**	**MN267740**	**MN313572**
N. formicarum	**INPA 2917** [a]	***Paullinia cupana***	**Brazil**	**MN267738**	**MN267741**	**MN313573**
N. formicarum	**INPA 2918** [a]	***Paullinia cupana***	**Brazil**	**MN267739**	**MN267742**	**MN313574**
N. acrostichi	MFLUCC 17-1754	*Acrostichum aureum*	Thailand	MK764272	MK764338	MK764316
N. acrostichi	MFLUCC 17-1755	*Acrostichum aureum*	Thailand	MK764273	MK764339	MK764317
N. brachiata	MFLUCC 17-1555	*Rhizophora apiculata*	Thailand	MK764274	MK764340	MK764318
N. petila	MFLUCC 17-1738	Rhizophora mucronata	Thailand	MK764275	MK764341	MK764319
N. petila	MFLUCC 17-1737	*Rhizophora mucronata*	Thailand	MK764276	MK764342	MK764320
N. rhizophorae	MFLUCC 17-1550	*Rhizophora mucronata*	Thailand	MK764277	MK764343	MK764321
N. rhizophorae	MFLUCC 17-1551	*Rhizophora mucronata*	Thailand	MK764278	MK764344	MK764322
N. sonneratae	MFLUCC 17-1745	*Sonneronata alba*	Thailand	MK764279	MK764345	MK764323
N. sonneratae	MFLUCC 17-1744	*Sonneronata alba*	Thailand	MK764280	MK764346	MK764324
N. thailandica	MFLUCC 17-1730	*Rhizophora mucronata*	Thailand	MK764281	MK764347	MK764325
N. thailandica	MFLUCC 17-1731	*Rhizophora mucronata*	Thailand	MK764282	MK764348	MK764326
N. alpapicalis	MFLUCC 17-2544	*Rhyzophora mucronata*	Thailand	MK357772	MK463545	MK463547
N. alpapicalis	MFLUCC 17-2545	symptomatic leaves *R. apiculate*	Thailand	MK357773	MK463546	MK463548
N. aotearoa	CBS 367.54	*Canvas*	New Zealand	KM199369	KM199454	KM199526
N. asiatica	MFLUCC 12-0286	unidentified tree	China	JX398983	JX399018	JX399049
N. australis	CBS 114159	*Telopea* sp.	Australia	KM199348	KM199432	KM199537
N. chrysea	MFLUCC 12-0261	dead leaves	China	JX398985	JX399020	JX399051
N. clavispora	MFLUCC 12-0281	*Magnolia* sp.	China	JX398979	JX399014	JX399045
N. cocoes	MFLUCC 15-0152	*Cocos nucifera*	Thailand	NR_156312	-	KX789689
N. coffea-arabicae	HGUP4015	*Coffea arabica*	China	KF412647	KF412641	KF412644
N. cubana	CBS 600.96	leaf litter	Cuba	KM199347	KM199438	KM199521
N. ellipsospora	MFLUCC 12-0283	dead plant material	China	JX398980	JX399016	JX399047
N. egyptiaca	CBS 140162	*Mangifera indica*	Egypt	KP943747	KP943746	KP943748
N. eucalypticola	CBS 264.37	*Eucalyptus globulus*	-	KM199376	KM199431	KM199551

.....continued on the next page

TABLE 2. (Continued)

Species	Strain number	Host	Country	ITS	*tub2*	*tef1-α*
N. foedans	CGMCC 3.9123	unidentified mangrove plant	China	JX398987	JX399022	JX399053
N. formicarum	CBS 362.72	dead ant	Ghana	KM199358	KM199455	KM199517
N. formicarum	CBS 115.83	Plant debris	Cuba	KM199344	KM199444	KM199519
N. formicarum	PSU-R-L02	*Hevea brasiliensis*	Thailand: Narathiwat	LC521861	LC521875	LC521869
N. formicarum	PSU-T-L01	*Hevea brasiliensis*	Thailand: Narathiwat	LC521858	LC521879	LC521873
N. formicarum	PSU-T-L02	*Hevea brasiliensis*	Thailand: Narathiwat	LC521859	LC521876	LC521870
N. formicarum	PSU-T-L05	*Hevea brasiliensis*	Thailand: Narathiwat	LC521856	LC521877	LC521871
N. honoluluana	CBS 114495	*Telopea* sp.	USA	KM199364	KM199457	KM199548
N. iraniensis	CBS 137768	*Fragaria* × *ananassa*	Iran	KM074048	KM074057	KM074051
N. javaensis	CBS 257.31	*Cocos nucifera*	Indonesia	KM199357	KM199457	KM199548
N. keteleeria	MFLUCC 13-0915	living leaves of *Keteleeria pubescens*	China	KJ503820	KJ503821	KJ503822
N. magna	MFLUCC 12-0652	*Pteridium* sp.	France	KF582795	KF582793	KF582791
N. mesopotamica	CBS 336.86	*Pinus brutia*	Iraq	KM199362	KM199441	KM199555
N. musae	MFLUCC 15-0776	*Musa* sp.	Thailand	NR_156311	KX789686	KX789685
N. natalensis	CBS 138.41	Acacia mollissima	South Africa	NR_156288	KM199466	KM199552
N. piceana	CBS 394.48	*Picea* sp.	UK	KM199368	KM199453	KM199527
N. piceana	CBS 254.32	Cocos nucifera	Indonesia	KM199372	KM199452	KM199529
N. piceana	CBS 225.3	Mangifera indica	-	KM199371	KM199451	KM199535
N. protearum	CBS 114178	*Leucospermum cuneiforme* cv. "Sunbird"	Zimbabwe	JN712498	KM199463	KM199542
N. protearum	CMM1357	-	-	KY549597	KY549632	KY549594
N. rosae	CBS 101057	*Rosa* sp.	New Zealand	KM199359	KM199429	KM199523
N. rosicola	CFCC 51992	*Rosa chinensis*	China	KY885239	KY885245	KY885243
N. rosicola	CFCC 51993	Rosa chinensis	China	KY885240	KY885246	KY885244
N. samarangensis	MFLUCC 12-0233	*Syzygium samarangense*	Thailand	JQ968609	JQ968610	JQ968611
N. saprophytica	MFLUCC 12-0282	*Magnolia* sp.	China	KM199345	KM199433	KM199538
N. steyaertii	IMI 192475	*Eucalyptus viminalis*	Australia	KF582796	KF582794	KF582792
N. surinamensis	CBS 450.74	soil under *Elaeis guineensis*	Suriname	KM199351	KM199465	KM199518
N. umbrinospora	MFLUCC 12-0285	unidentified plant	China	JX398984	JX399019	JX399050
N. vitis	MFLUCC 15-1265	*Vitis vinifera* cv. "Summer black"	China	KU140694	KU140685	KU140676
N. zimbabwana	CBS 111495	*Leucospermum cunciforme* cv. "Sunbird"	Zimbabwe	JX556231	KM199456	KM199545

[a] INPA—National Institute of Amazon Research.

The phylogenetic inference in *Pseudopestalotiopsis* was performed using the new sequences generated in the current study with sequences uploaded from NCBI (http: //www.ncbi.nlm.nih) of the other 20 members of the *Pseudopestalotiopsis* genus. The sequences of *Neopestalotiopsis formicarum* were used as outgroup. The phylogenetic inference in *Neopestalotiopsis* was conducted with sequences uploaded from NCBI (http: //www.ncbi.nlm.nih) of 38 members of the genus, the new sequences generated in the current study and sequences of *Pestalotiopsis diversiseta*

as outgroup. For each locus, sequences were aligned using the MUSCLE algorithm and manually edited. Phylogenetic analysis was performed using concatenated sequences of the three loci (ITS, *tub2* and *tef1-α*) using maximum likelihood (ML), maximum parsimony (MP) and Bayesian inference (BI). For ML, a Tamura-Nei model with distributed Range (G) rates was adopted, while for MP a cut-off limit of 95% was established, and a nonparametric bootstrap was done with 1000 replicates. Both ML and MP were performed using MEGA 7 (Kumar *et al.* 2016). BI was based on the model tested by PAUP*4 and Mrmodeltest2 v2 (Nylander 2004). All sites sequenced at the ITS, *tub2 and tef1-α* were considered, and the analysis was run for ten million generations, with the first 25% of trees discarded as burn-in, using the MrBayes v 3.6 tool available at CIPRES (https://www.phylo.org/). Posteriori probability (PP) and tree topology were visualized with Figtree v 1.3.1 (Rambaut 2009).

Pathogenicity in guarana plant and other economically important hosts

Pathogenicity assay was conducted in four-year-old guarana plants under field conditions. Conidial suspension of the strains: INPA 2913, INPA 2914, INPA 2915, INPA 2916, INPA 2917 and INPA 2918 were prepared using a concentration of 1×10^6 conidia/mL. Conidial suspensions were sprayed on leaves of guarana plants previously injured by needles. Uninoculated guarana plants sprayed with sterile distilled water served as the negative control. The pathogenicity assays were conducted in triplicate. Three to four days after spraying, and based on a set of symptoms, re-isolation was performed and pathogenicity was verified by fulfillment of Koch's postulate.

Subsequently, a pathogenicity assay with the same six strains was also performed with a broad range of economically important tropical hosts, under greenhouse conditions. Inoculation was performed on seedlings of açaí palms (*Euterpe oleracea* Mart. and *E. precatoria* Mart.), oil palm plants (*Elaeis guineensis* Jacq.), banana (*Musa paradisiaca* var. pavocan) and rubber trees (*Hevea brasiliensis*). The pathogenicity assay was conducted as the one performed on the guarana plants. Uninoculated plants sprayed with sterile distilled water served as negative control while guarana plants were used as a positive control to confirm the viability of the inoculum. The pathogenicity assay was conducted in triplicate. Two to seven days after spraying, and based on a set of symptoms, re-isolation was performed, and pathogenicity was verified by fulfillment of Koch's postulate. The greenhouse experiments were repeated under the same conditions, to confirm the results.

Results

Phylogenetic analyses

The alignment of concatenated sequences of ITS, *tub2 and tef1-α* loci used for phylogenetic inference in *Pseudopestalotiopsis,* consisted of sequences of the 20 *Pseudopestalotiopsis* species, sequences of three new strains (INPA 2913, INPA 2914 and INPA 2915) isolated from the guarana plant, and sequences of the outgroup *N. formicarum* (Table 2). The resulting dataset consisted of 1865 characters (ITS: 536, *tub2*: 812 and *tef1-α*: 517) including gaps. For *tef1-α*, the best fitting model selected by AIC in MrModeltest2 was GTR+I+G, while for ITS and *tub2*, the model HKY+G was selected. The phylogenetic tree of the new strains of *Pseudopestalotiopsis* (INPA 2913, INPA 2914 and INPA 2915) was placed in the clade containing three species: *Ps. thailandica, Ps. rhizophorae and Ps. simitheae* (Figure 1).

For the phylogenetic inference in *Neopestalotiopsis,* alignment of the concatenated sequences of ITS, *tub2* and *tef1-α* loci, were performed with sequences of the 38 members. The three new strains (INPA 2916, INPA 2917 and INPA 2918) isolated from the guarana plant, were identified as *N. formicarum* (Figure 2). The resulting dataset comprises 1604 characters (ITS: 452, *tub2*: 785 and *tef1-α*: 367) including gaps. For ITS, the best fitting model selected by AIC in MrModeltest2 was GTR+G, while HKY+G for *tub2* and *tef1-α*.

Taxonomy and Morphology

***Pseudopestalotiopsis gilvanii* INPA 2913** Silva, Gilvan F.; Gualberto, Gilvana F.; Catarino, Aricleia M., Fernandes, Thiago S., *sp. nov.* MycoBank: MB837806

TABLE 3. Morphological characteristics of the strains of *Pseudopestalotiopsis gilvanii* and *Neopestalotiopsis formicarum* of this study and description of others known pestalotioid species.

Species	Conidium size (µm)	Apical appendage		Basal appendage	Colony morphology		References
		N°	*Length (µm)*		*Top color*	*Reverse*	
Pseudopestalotiopsis dawaina	22–31 x 8–9.5	3	20.5–33.5	Present	Whitish to pinkish	Dark brown	(Nozawa *et al.* 2018)
Ps. dawaina INPA 2909	20.4–28.3 x 5.4–9.5	2–3	17.5–32.6	Present	Whitish to pinkish	White to dark brown	(Catarino *et al.* 2020)
Ps. dawaina INPA 2912	20–30 x 6.2–7.9	2–3	17.9–29.3	Present	White	White to dark brown	(Catarino *et al.* 2020)
Ps. simitheae	22–30 x 5–6.5	2–4	14.5–26.5	Present	White	Orange	(Song *et al.* 2014)
Ps. rhizophorae	22–25 x 6.5–7	1–2	20–29	Present	White	White	(Maharachchikumbura *et al.* 2014)
Ps. thailandica	24.5–30 x 5.5–6	1–3	28–36	Present	White	White	(Maharachchikumbura *et al.* 2014)
***Ps. gilvanii* INPA 2913**	**24–34.3 x 4.6–7.3**	**2–5**	**14.8–39.9**	**Present**	**White**	**White**	**Present study**
***Ps. gilvanii* INPA 2914**	**21.2–32.9 x 5–7.5**	**2–5**	**14.9–40.9**	**Present**	**White**	**White**	**Present study**
***Ps. gilvanii* INPA 2915**	**24.2–32.6 x 4.7–7**	**2–5**	**15–40.8**	**Present**	**White**	**White**	**Present study**
Neopestalotiopsis formicarum	21–28 x 7.5–9.5	2–3	23–33	Present	Whitish to pale honey	Whitish to pale honey	(Maharachchikumbura *et al.* 2014)
***N. formicarum* INPA 2916**	**19.7–27.8 x 5.5–7.5**	**2–3**	**10–23.7**	**Present**	**Whitish to pale honey**	**Whitish to pale honey**	**Present study**
***N. formicarum* INPA 2917**	**18.8–28.9 x 5–7**	**2–3**	**21.4–23.2**	**Present**	**White**	**White**	**Present study**
***N. formicarum* INPA 2918**	**22–30 x 5–6.5**	**2–3**	**17.1–28.1**	**Present**	**White**	**White**	**Present study**

***Etymology*:** Refers to the first name of the author who designed this study.

***Holotype*:** INPA 2913

Pycnidial conidiomata on PDA, fusiform, ellipsoid or straight. Concolourous conidia measuring 24.02–34.28 × 4.63–7.35 µm, 3–5 septa and 2–5 appendages of 14.86–39.92 µm long (Table 3; Figure 3A–C). This strain differs from *Ps. simitheae* by *tef1-α* (9-bp) and *tub2* (27 bp) sequence data (Figure 4).

***Culture characteristics*:** Colonies on PDA with 95 mm of diameter after 7 days at a room temperature of ± 25 °C. Coloration: white with cottony and vigorous aerial mycelium. Numerous black pycnidia in the center of the colony of reverse white with black dots (Table 3; Figure 3A).

***Material examined*:** Brazil, Amazonas State, Manaus, on leaves of guarana plants (*Paullinia cupana* var. *sorbilis*), 11 Sep. 2017, G. F. Gualberto, INPA 2913 (holotype), ex-type living culture (INPA 2013).

Neopestalotiopsis formicarum S.S.N. Maharachchikumbura, K.D. Hyde & P.W. Crous, Studies in Mycology 79: 121. 2104

Conidia comprise five cells (19.7–27.8 × 5.5–7.5 µm) with 3–5 septa and 2–3 appendages (10–23.7 µm). The colony was whitish to pale honey, vigorous and cottony mycelium. Median cell was versicolor with staining ranging from olive brown to dark brown. Intense conidia production in PDA medium was also observed by SEM (Table 3, Figure 3D–F).

***Material examined*:** Brazil, Amazonas State, Manaus, on leaves of guarana plants (*Paullinia cupana* var. *sorbilis*), 11 Sep. 2017, G. F. Gualberto, ex-type culture (INPA 2916).

Pathogenicity in guarana plant and other economically important hosts

Leaves of guarana plants inoculated with isolates of *Ps. gilvanii* and *N. formicarum* developed necrotic spots within 3–4 days after inoculation (Figure 5C and 5E). The necrosis expands to the foliar limb causing the fall of the leaves (Figure 5G–H). Control remains asymptomatic (Figure 5A-B). Once the pathogenicity assay was conducted under field conditions and due to the similarity between anthracnose symptoms caused by *C. guaranicola,* and leaf spot symptoms caused by pestalotioid fungi, scanning electron microscopy was adopted, which detected only the presence of conidia of *Ps. gilvanii* and *N. formicarum* (Figure 5D and 5F). The Koch's postulate was completed by re-isolation from inoculated guarana plant leaves.

The necrotic spot symptoms observed in guarana leaves were reproduced in açaí palms (*E. oleracea* and *E. precatoria*) and oil palm (*E. guineensis*). In banana (*M. paradisiaca* var. *pacovan*), the necrotic spot symptoms were observed after inoculation with *N. formicarum,* while the absence of symptoms was observed after inoculation with *Ps. gilvanii*. In rubber trees (*H. brasiliensis*), the absence of symptoms was also observed after inoculation with *Ps. gilvanii* and *N. formicarum* (Figure 6). To confirm the pathogenicity of the fungal species in these crops, we re-isolated from the observed symptoms, concluding all stages of Koch's postulate. The results are summarized in Table 4.

TABLE 4. Summary of pathogenicity of *Pseudopestalotiopsis gilvanii* and *Neopestalotiopsis formicarum* for six tropical plant species.

Botanical species	Fungal species	
	Pseudopestalotiopsis gilvanii	***Neopestalotiopsis formicarum***
	Symptoms	
Paullinia cupana	+	+
Euterpe oleraceae	+	+
Euterpe precatoria	+	+
Elaeis guineenses	+	+
Musa paradisiaca	-	+
Hevea brasiliensis	-	-

Discussion

After six years of taxonomy restructuring of pestalotioid fungi by Maharachchikumbura *et al.* (2014), the number of species in *Pseudopestalotiopsis* increased from 3 to 22 (http://www.indexfungorum.org/). In the present study, six fungal isolates obtained from necrotic spots on guarana leaves were identified with combine morphological examination and multi-locus phylogenetic analysis of ITS*, tub2* and *tef1-α* regions. The three strains (INPA 2913, INPA 2914 and INPA 2915) were proposed as a new species named *Pseudopestalotiopsis gilvanii* and the other three strains (INPA 2916, INPA 2917 and INPA 2918) were identified as *N. formicarum*. Phylogenetic inference in *Pseudopestalotiopsis* placed *Ps. gilvanii* basal to a clade composed by *Ps. thailandica*, *Ps. rhizophorae* and *Ps. simitheae*. The differences between the nucleotides of *Ps. gilvanii* and *Ps. thailandica* (ITS: 1.43%, *tub2*: 4.26% and *tef1-α*: 2.16%); *Ps. gilvanii* and *Ps. simitheae* (ITS: 0.82%, *tub2*: 3.4% and *tef1-α*: 1.74%); *Ps. gilvanii* and *Ps. rhizophorae* (ITS: 0.37%, *tub2*: 3.06% and *tef1-α*: 1.55%) supported *Ps. gilvanii* as a new taxon, as recommended by Jeewon & Hyde (2016). Further, *Ps. gilvanii* can also be differentiated from *Ps. thailandica, Ps. simitheae and Ps. rhizophorae* by longer conidium length, higher number of apical appendage (Table 3) and by outstanding nucleotide differences in *tub2*, only one out of 28 nucleotides were shared by the closely related *Ps. gilvanii* and *Ps. simitheae*.

Six strains of *N. formicarum* have been reported to date (Maharachchikumbura *et al.* 2014; Pornsuriya *et al.* 2020). The four most recently described as *N. formicarum* were isolated from rubber trees in Thailand (Pornsuriya *et al.* 2020). These strains formed a clade related to *N. formicarum* (CBS 362.72 and CBS 115.83), but with low bootstrap support. The addition of the new strains from the current study better resolved the *N. formicarum* clade compared to the phylogenetic tree previously reported (Pornsuriya *et al.* 2020). Our isolates clustered with CBS 362.72 and CBS 115.83, while the ones obtained from rubber trees formed a distinct clade, suggesting that the Thailand isolates may be a new species. This hypothesis is also reinforced by contrasting results related to pathogenicity between isolates identified as *N. formicarum* in Thailand and Brazil. The ones from Thailand were pathogenic to rubber trees while the ones from Brazil were not.

The *N. formicarum* species has so far been reported as a saprophyte on plant debris and dead ants (Maharachchikumbura *et al.* 2014). Here, we presented *N. formicarum* as a broad-spectrum plant pathogen, able to cause leaf spots on guarana plant, açai palms (*E. oleraceae* and *E. precatoria*), banana and oil palm. Switching, from saprophytic to pathogenic lifestyle, has been reported among other saprophytic species revealing emergent plant pathogens with a potential impact on crop production (Fisher *et al.* 2012; Fones & Gurr 2017; Karim *et al.* 2016). Our study on pestalotioid fungi shows plant pathogens that could decrease crop production due to a severe set of symptoms, starting with necrotic spots and progressing to defoliation, as observed in guarana plant (Figure 5G-H). Therefore, identification and characterization of new plant pathogens are crucial to the establishment of an efficient disease-management strategy.

The tropical crops evaluated here already suffer from diseases caused by other fungi. Decades have been spent on research to mitigate their impact, by the development of disease-management plans, and breeding to improve pathogen resistance. The well-known threats to the banana are *Fusarium oxysporum* f. sp. *cubense* (Foc), which causes Fusarium wilt and *Pseudocercospora fijiensis*, which cause black Sigatoka (Chen *et al.* 2019; Churchill 2011). Açaí palms are attacked by the *Colletotrichum* species (Castro *et al.* 2017), while the oil palm is attacked by *Ganoderma boninense, Curvularia oryzae* and *Phytophthora palmivora* (Chong *et al.* 2017; Sunpapao *et al.* 2014; Torres *et al.* 2016).

The main guarana plant pathogens are *C. guaranicola* and *F. decemcellulare* (Queiroz *et al.* 2020) and the Brazilian breeding program has worked with released cultivars, resistant to them. However, the pestalotioid fungi reported here were isolated from guarana clones improved for yield and resistance*,* thus making them the newest risk to guarana plant production in Brazil and efforts must be taken to prevent the disease from spreading to other guarana growing locations.

The multi-host ability of *Ps. gilvanii* and *N. formicarum* demonstrates the potential risk to important tropical crops. The understanding of molecular mechanisms of pathogenicity and virulence are critical to the development of disease control strategies. Our research team is currently working on the whole genome sequence analysis to provide new insight into the molecular mechanisms of virulence and pathogenicity in pestalotioid fungi described here.

Acknowledgment

This study was financed in part by the Coordenação de Aperfeiçoamento de Pessoal de Nível Superior—Brasil (CAPES)—Finance Code (88887.200468/2018-00)—PROCAD/AmazonMicro, Amazonas State Research Foundation (FAPEAM)—Amazonas Estratégico and National Council for Scientific and Technological Development (CNPq). AMC thank the Coordenação de Aperfeiçoamento de Pessoal de Nível Superior—CAPES for a scholarship. The authors thank Dr. Ricardo Lopes, Dr. Ewerton Rabelo Cordeiro and Dr. Firmino José do Nascimento Filho of Embrapa Amazônia Ocidental for the supply of seedlings of palm, rubber and guarana trees. The authors also wish to thank José Wilson dos Santos Meirelles, Lucas Castanhola Dias and Jackieline Souza Veras Lima of National Institute of Amazon Research for their support on Scanning Electron Microscopy analysis.

References

Alade, G.O., Moody, J.O., Bakare, A.G., Awotona, O.R., Adesanya, S., Lai, D., Debbab, A. & Proksch, P. (2018) Metabolites from endophytic fungus; *Pestalotiopsis clavispora* isolated from *Phoenix reclinata* leaf. *Future Journal of Pharmaceutical Sciences* 4: 273–275.
https://doi.org/10.1016/j.fjps.2018.10.001

Ayoubi, N. & Pari, S.S. (2016) Morphological and molecular identification of *Neopestalotiopsis mesopotamica* causing tomato fruit rot. *Journal of Plant Diseases and Protection* 123: 267–271.
https://doi.org/10.1007/s41348-016-0042-z

Ayoubi, N. & Soleimani, M.J. (2016) Strawberry fruit rot caused by *Neopestalotiopsis iranensis sp. nov.*, and *N. mesopotamica*. *Current Microbiology* 72: 329–336.
https://doi.org/10.1007/s00284-015-0955-y

Beaufort, B. (2018) La mercatique transatlantique d'un végétal psychoactif, le guaraná, entre remède et alimente (1840-1921). *Confins* 35: 1–25.
https://doi.org/10.4000/confins.13215

Bonadiman, B. da S.R., Cadoná, F.C., Assmann, C.E., Weis, G.C.C., Alves, A. de O., Duarte, M.F., Chaves, C.M., Chaves, C. do C., Motta, K.M. dos S., Ribeiro, E.E., Bagatini, M.D. & Cruz, I.B.M. (2017) Guarana (*Paullinia cupana*): Cytoprotective effects on age-related eye dysfunction. *Journal of Functional Foods* 36: 375–386.
https://doi.org/10.1016/j.jff.2017.07.027

Carbone, I. & Kohn, L.M. (1999) A method for designing primer sets for speciation studies in filamentous ascomycetes. *Mycologia* 91: 553–556.
https://doi.org/10.1080/00275514.1999.12061051

Carvalho, L.V. do N., Cordeiro, M.F., Line e Lins, T.U., Sampaio, M.C.P.D., Mello, G.S.V. de, Costa, V. de C.M., Marques, L.L.M., Klein, T., Mello, J.C.P. de, Cavalcanti, I.M.F., Pitta, I. da R., Pitta, M.G. da R. & Rêgo, M.J.B. de M. (2016) Evaluation of antibacterial, antineoplastic, and immunomodulatory activity of *Paullinia cupana* seeds crude extract and ethyl-acetate fraction. *Evidence-Based Complementary and Alternative Medicine* 2016: 1–7.
https://doi.org/10.1155/2016/1203274

Castro, G.L.S., Júnior, D.D.S., Bueno, A.C.S.O., Silva, G.B. & Silva, G.B. (2017) Anthracnose in açaí palm leaves reduces leaf gas exchange and chlorophyll a fluorescence. *Tropical Plant Pathology* 42: 13–20.
https://doi.org/10.1007/s40858-016-0118-0

Catarino, A. de M., Hanada, R.E., Queiroz, C.A. de, Sousa, T.F., Lima, Í.N., Gasparotto, L. & Silva, G.F. da (2020) First report of *Pseudopestalotiopsis dawaina* causing spots in *Caryota mitis* in Brazil. *Plant Disease* 104: 989.
https://doi.org/10.1094/PDIS-08-19-1771-PDN

Chen, A., Sun, J., Matthews, A., Armas-Egas, L., Chen, N., Hamill, S., Mintoff, S., Tran-Nguyen, L.T.T., Batley, J. & Aitken, E.A.B. (2019) Assessing variations in host resistance to *Fusarium oxysporum* f sp. *cubense* Race 4 in *Musa* species, with a focus on the subtropical Race 4. *Frontiers in Microbiology* 10: 1–13.
https://doi.org/10.3389/fmicb.2019.01062

Chen, Y., Zeng, L., Shu, N., Jiang, M., Wang, H., Huang, Y. & Tong, H. (2018) *Pestalotiopsis*-like species causing gray blight disease on *Camellia sinensis* in China. *Plant Disease* 102: 98–106.
https://doi.org/10.1094/PDIS-05-17-0642-RE

Chong, K.P., Dayou, J. & Alexander, A. (2017) *Detection and control of Ganoderma boninense in oil palm crop.* SpringerBriefs in Agriculture, pp. 5–13.
https://doi.org/10.1007/978-3-319-54969-9_2

Churchill, A.C.L. (2011) Pathogen profile *Mycosphaerella fijiensis,*, the black leaf streak pathogen of banana: progress towards understanding pathogen biology and detection, disease development, and the challenges of control. *Molecular Plant Pathology* 12: 307–328.
https://doi.org/10.1111/j.1364-3703.2010.00672.x

Cord-Landwehr, S., Melcher, R.L.J., Kolkenbrock, S. & Moerschbacher, B.M. (2016) A chitin deacetylase from the endophytic fungus *Pestalotiopsis* sp. efficiently inactivates the elicitor activity of chitin oligomers in rice cells. *Scientific Reports* 6: 1–11.
https://doi.org/10.1038/srep38018

Costa, L.A. & Gusmão, L.F.P. (2015) Characterization saprobic fungi on leaf litter of two species of trees in the Atlantic Forest, Brazil. *Brazilian Journal of Microbiology* 46: 1027–1035.
https://doi.org/10.1590/S1517-838246420140548

Doyle, J. & Doyle, J. (1990) Isolation of plant DNA from fresh tissue. *Focus* 12: 13–15.
https://doi.org/10.2307/2419362

Fisher, M.C., Henk, D.A., Briggs, C.J., Brownstein, J.S., Madoff, L.C., McCraw, S.L. & Gurr, S.J. (2012) Emerging fungal threats to animal, plant and ecosystem health. *Nature* 484: 186–194.
https://doi.org/10.1038/nature10947

Fones, H.N. & Gurr, S.J. (2017) NOXious gases and the unpredictability of emerging plant pathogens under climate change. *BMC Biology* 15: 1–9.
https://doi.org/10.1186/s12915-017-0376-4

Glass, N.L. & Donaldson, G.C. (1995) Development of primer sets designed for use with the PCR to amplify conserved genes from filamentous ascomycetes. *Applied and Environmental Microbiology* 61: 1323–1330.
https://doi.org/10.1128/AEM.61.4.1323-1330.1995

Hlaiem, S., Zouaoui-boutiti, M., Lahbib, M., Jemâa, B., Carthage, U. De, Karray, R.H., Rocca, G. Della, Barberini, S., Danti, R., Ipsp-cnr, P.P. & Madonna, V. (2018) Identification and pathogenicity of *Pestalotiopsis chamaeropis*, causal agent of white heather (*Erica arborea*) dieback, and in vitro biocontrol with the antagonist *Trichoderma* sp . *Tunisian Journal of Plant Protection* 13: 49–60.

Jayawardena, R.S., Liu, M., Maharachchikumbura, S.S.N., Zhang, W., Xing, Q., Hyde, K.D., Nilthong, S., Li, X. & Yan, J. (2016) *Neopestalotiopsis vitis sp. nov.* causing grapevine leaf spot in China. *Phytotaxa* 258: 63–74.
https://doi.org/10.11646/phytotaxa.258.1.4

Jeewon, R. & Hyde, K.D. (2016) Establishing species boundaries and new taxa among fungi: Recommendations to resolve taxonomic ambiguities. *Mycosphere* 7: 1669–1677.
https://doi.org/10.5943/mycosphere/7/11/4

Jeewon, R., Ittoo, J., Mahadeb, D., Jaufeerally-Fakim, Y., Wang, H.-K. & Liu, A.-R. (2013) DNA based identification and phylogenetic characterisation of endophytic and saprobic fungi from *Antidesma madagascariense*, a medicinal plant in Mauritius. *Journal of Mycology* 2013: 1–10.
https://doi.org/10.1155/2013/781914

Jeewon, R., Liew, E.C.Y. & Hyde, K.D. (2002) Phylogenetic relationships of *Pestalotiopsis* and allied genera inferred from ribosomal DNA sequences and morphological characters. *Molecular Phylogenetics and Evolution* 25: 378–392.
https://doi.org/10.1016/S1055-7903(02)00422-0

Jeewon, R., Liew, E.C.Y., Simpson, J.A., Hodgkiss, I.J. & Hyde, K.D. (2003) Phylogenetic significance of morphological characters in the taxonomy of *Pestalotiopsis* species. *Molecular Phylogenetics and Evolution* 27: 372–383.
https://doi.org/10.1016/S1055-7903(03)00010-1

Karim, N.F.A., Mohd, M., Nor, N.M.I.M. & Zakaria, L. (2016) Saprophytic and potentially pathogenic *Fusarium* species from peat soil in perak and pahang. *Tropical Life Sciences Research* 27: 1–20.

Kathiravan, G., Sri Raman, V., Rajangam, B. & Rajasekar, A. (2014) Infra-red spectral analysis of taxol produced by different species of *Pestalotiopsis*. *Journal of Analytical & Bioanalytical Techniques* 5: 1–9.
https://doi.org/10.4172/2155-9872.1000205

Klaiklay, S., Rukachaisirikul, V., Tadpetch, K., Sukpondma, Y., Phongpaichit, S., Buatong, J. & Sakayaroj, J. (2012) Chlorinated chromone and diphenyl ether derivatives from the mangrove-derived fungus *Pestalotiopsis* sp. PSU-MA69. *Tetrahedron* 68: 2299–2305.
https://doi.org/10.1016/j.tet.2012.01.041

Kumar, S., Stecher, G. & Tamura, K. (2016) MEGA7: Molecular evolutionary genetics analysis version 7.0 for bigger datasets. *Molecular biology and evolution* 33: 1870–1874.
https://doi.org/10.1093/molbev/msw054

Liu, H., Liu, S., Guo, L., Zhang, Y., Cui, L. & Ding, G. (2012) New furanones from the plant endophytic fungus *Pestalotiopsis besseyi*. *Molecules* 17: 14015–14021.
https://doi.org/10.3390/molecules171214015

Maharachchikumbura, S.S.N., Hyde, K.D., Groenewald, J.Z., Xu, J. & Crous, P.W. (2014) *Pestalotiopsis* revisited. *Studies in Mycology* 79: 121–186.
https://doi.org/10.1016/j.simyco.2014.09.005

Marzall-Pereira, M., Savi, D.C., Bruscato, E.C., Niebisch, C.H., Paba, J., Aluízio, R., Ferreira-Maba, L.S., Galli-Terasawa, L.V., Glienke, C. & Kava, V. (2019) *Neopestalotiopsis* species presenting wide dye destaining activity: report of a mycelium-associated laccase. *Microbiological Research* 228: 126299.
https://doi.org/10.1016/j.micres.2019.126299

Morales-Rodríguez, C., Dalla Valle, M., Aleandri, M.P. & Vannini, A. (2019) *Pestalotiopsis biciliata*, a new leaf pathogen of *Eucalyptus,* spp. recorded in Italy. *Forest Pathology* 49: 1–7.
https://doi.org/10.1111/efp.12492

Norphanphoun, C., Jayawardena, R.S., Chen, Y., Wen, T.C., Meepol, W. & Hyde, K.D. (2019) Morphological and phylogenetic characterization of novel pestalotioid species associated with mangroves in Thailand. *Mycosphere* 10: 531–578.
https://doi.org/10.5943/mycosphere/10/1/9

Nozawa, S., Ando, K., Phay, N. & Watanabe, K. (2018) *Pseudopestalotiopsis dawaina sp. nov.* and *Ps. kawthaungina sp. nov.*: two new species from Myanmar. *Mycological Progress* 17: 865–870.
https://doi.org/10.1007/s11557-018-1398-1

Nylander, J.A.A. (2004) MrModeltest v2. Program distributed by the author. *Evolutionary Biology Centre Uppsala University*.

O'Donnell, K. & Cigelnik, El. (1997) Two divergent intragenomic rDNA ITS2 types within a monophyletic lineage of the fungus *Fusarium* are nonorthologous. *Molecular Phylogenetics and Evolution* 7: 103–116.
https://doi.org/10.1006/mpev.1996.0376

O'Donnell, K., Kistler, H.C., Gigelnik, E. & Ploetz, R.C. (1998) Multiple evolutionary origins of the fungus causing Panama disease of banana: Concordant evidence from nuclear and mitochondrial gene genealogies. *PNAS* 95: 2044–2049.
https://doi.org/10.1073/pnas.95.5.2044

Pornsuriya, C., Chairin, T., Thaochan, N. & Sunpapao, A. (2020) Identification and characterization of *Neopestalotiopsis* fungi associated with a novel leaf fall disease of rubber trees (*Hevea brasiliensis*) in Thailand. *Journal of Phytopathology*: 416–427.
https://doi.org/10.1111/jph.12906

Queiroz, C.A. de, Matos, K. da S., Lobo, I.K.C., Sousa, S.B. de, Muniz, C.R., Yamagishi, M.E.B., Zocolo, G.J., Hanada, R.E., Gasparotto, L., Sousa, N.R., Andrade, E.V. de, Cordeiro, I.B., Melo, A.A.M. & Silva, G.F. da (2020) Morpho-anatomical and molecular characterization of the oversprouting symptoms caused by *Fusarium decemcellulare* in guarana plants (*Paullinia cupana* var. *sorbilis*). *Tropical Plant Biology* 13: 274–286.
https://doi.org/10.1007/s12042-020-09256-1

Rambaut, A. (2009) FigTree v1.3.1: Tree figure drawing tool. *PeerJ* 2: e281.

Rangel, M.P., Mello, J.C.P. De & Audi, E.A. (2013) Evaluation of neurotransmitters involved in the anxiolytic and panicolytic effect of the aqueous fraction of *Paullinia cupana* (guaraná) in elevate T maze. *Revista Brasileira de Farmacognosia* 23: 358–365.
https://doi.org/10.1590/S0102-695X2013005000024

Riga, R., Happyana, N. & Hakim, E.H. (2019) Chemical Constituents of *Pestalotiopsis microspora* HF 12440. *Journal of Applied Pharmaceutical Science* 9: 108–124.
https://doi.org/10.7324/JAPS.2019.90116

Russell, J.R., Huang, J., Anand, P., Kucera, K., Sandoval, A.G., Dantzler, K.W., Hickman, D.S., Jee, J., Kimovec, F.M., Koppstein, D., Marks, D.H., Mittermiller, P.A., Núñez, S.J., Santiago, M., Townes, M.A., Vishnevetsky, M., Williams, N.E., Vargas, M.P.N., Boulanger, L.A., Bascom-Slack, C. & Strobel, S.A. (2011) Biodegradation of polyester polyurethane by endophytic fungi. *Applied and Environmental Microbiology* 77: 6076–6084.
https://doi.org/10.1128/AEM.00521-11

Shu, J., Yu, Z., Sun, W., Zhao, J., Li, Q., Tang, L., Guo, T., Huang, S., Mo, J., Hsiang, T. & Luo, S. (2020) Identification and characterization of pestalotioid fungi causing leaf spots on mango in southern China. *Plant Disease* 104: 1207–1213.
https://doi.org/10.1094/PDIS-03-19-0438-RE

Silveira, A.K., Moresco, K.S., Gomes, H.M., Morrone, M. da S., Grun, L.K., Gelain, D.P., Pereira, L. de M., Giongo, A., Oliveira, R.R. de & Moreira, J.C.F. (2018) Guarana (*Paullinia cupana* Mart.) alters gut microbiota and modulates redox status, partially via caffeine in Wistar rats. *Phytotherapy Research* 32: 2466–2474.
https://doi.org/10.1002/ptr.6185

Song, Y., Tangthirasunun, N., Maharachchikumbura, S.S.N., Jiang, Y., Xu, J., Hyde, K.D. & Wang, Y. (2014) Novel *Pestalotiopsis* species from Thailand point to the rich undiscovered diversity of this chemically creative genus. *Cryptogamie, Mycologie* 35: 139–149. https://doi.org/10.7872/crym.v35.iss2.2014.139

Sunpapao, A., Kittimorakul, J. & Pornsuriya, C. (2014) Disease Note: Identification of *Curvularia oryzae* as cause of leaf spot disease on oil palm seedlings in nurseries of Thailand. *Phytoparasitica* 42: 529–533. https://doi.org/10.1007/s12600-014-0390-9

Torres, G.A., Sarria, G.A., Martinez, G., Varon, F., Drenth, A. & Guest, D.I. (2016) Bud rot caused by *Phytophthora palmivora*: A destructive emerging disease of oil palm. *Phytopathology* 106: 320–329. https://doi.org/10.1094/PHYTO-09-15-0243-RVW

Tsai, I., Chung, C., Lin, S., Hung, T., Shen, T.-L., Hu, C.-Y., Hossein, W.N. & Ariyawansa, H.A. (2020) Cryptic diversity, molecular systematics and pathogenicity of *Pestalotiopsis* and allied genera causing grey blight disease of tea in Taiwan, with description of a new species of *Pseudopestalotiopsis*. *Plant Disease*. https://doi.org/10.1094/PDIS-05-20-1134-RE

Wang, Y., Ran, S.F., Maharachchikumbura, S.S.N., Al-Sadi, A.M., Hyde, K.D., Wang, H.L., Wang, T. & Wang, Y.X. (2017) A novel *Pestalotiopsis* species isolated from *Bulbophyllum thouars* in Guangxi Province, China. *Phytotaxa* 306: 96–100. https://doi.org/10.11646/phytotaxa.306.1.9

White, T., Bruns, T., Lee, S. & Taylor, J. (1990) Amplification and direct sequencing of fungal ribosomal RNA genes for phylogenetics. *In:* Innis, M.A., Gelfand, D.H., Sninsky, J.J. & White, T. (Eds.) *PCR protocols: a guide to methods and applications*. Academic Press (Elsevier), Amsterdam, pp. 315–322. https://doi.org/10.1016/B978-0-12-372180-8.50042-1

Xu, J., Ebada, S.S. & Proksch, P. (2010) *Pestalotiopsis* a highly creative genus: Chemistry and bioactivity of secondary metabolites. *Fungal Diversity* 44: 15–31. https://doi.org/10.1007/s13225-010-0055-z

Yu, X., Müller, W.E.G., Meier, D., Kalscheuer, R., Guo, Z., Zou, K., Umeokoli, B.O., Liu, Z. & Proksch, P. (2020) Polyketide derivatives from mangrove derived endophytic fungus *Pseudopestalotiopsis theae*. *Marine Drugs* 18: 1–15. https://doi.org/10.3390/md18020129

Yuan, C., Ding, G., Wang, H.Y., Guo, Y.H., Shang, H., Ma, X.J. & Zou, Z.M. (2017) Polyketide-terpene hybrid metabolites from an endolichenic fungus *Pestalotiopsis* sp. *BioMed Research International* 2017. https://doi.org/10.1155/2017/6961928

Zhao, J., Zhang, D., Liu, T., Liu, W., Pan, L., Liao, N. & Liu, D. (2020) First report of *Pseudopestalotiopsis* and *Neopestalotiopsis* species causing leaf spot of *Camellia chrysantha* in China. *Plant Disease*: 3–5. https://doi.org/10.1094/PDIS-03-20-0598-PDN

Zhou, J., Diao, X., Wang, T., Chen, G., Lin, Q., Yang, X. & Xu, J. (2018) Phylogenetic diversity and antioxidant activities of culturable fungal endophytes associated with the mangrove species *Rhizophora stylosa* and *R. mucronata* in the South China Sea. *PLoS ONE* 13. https://doi.org/10.1371/journal.pone.0197359